Urol Res (1999) 27:462–469

ORIGINAL PAPER

George A. Barbalias · George Nikiforidis
Pavlos Vassilakos · Evangelos N. Liatsikos

Obstructive uropathy versus nephropathy: compartmental analysis in radioisotopic renography as a new methodology

Received: 3 November 1998 / Accepted: 11 March 1999

Abstract A study was carried out to determine the spatial-temporal distribution of the radiopharmaceutical, ^{99m}Tc-DTPA in the kidney and its compartments during renography and the use of compartmental analysis to improve the diagnostic capability of renography. A total of 60 individuals formed three groups: group A consisted of 30 normals taken as controls, group B consisted of 15 patients with unilateral nephropathy, and group C consisted of 15 patients with unilateral obstructive uropathy. This retrospective study was performed by processing of the frames acquired in the various stages of renography and determination of the time distribution of radioactivity in the aorta, the renal parenchyma and the renal pelvis. The data acquired were used to produce three curves instead of one for each kidney and to study renal function as a system of six compartments (aorta, left and right renal parenchyma, left and right renal pelvis, and bladder). In all the above compartments the differences among the three groups were significant and were quantified using the flow coefficients of the aortorenal compartments. The differences between the aortic flow coefficients (k_1) were statistically significant not only between normal controls and patients, but also between individuals with parenchymatic dysfunction and patients with pelvocalyceal obstruction. The same differences were seen comparing the pelvocalyceal coefficients (k_3) of all three groups. The parenchymatic coefficient (k_2) presented statistically significant differences between normals and patients which were not observed between the two groups of patients (B and C). Compartmental analysis thus increases the sensitivity of renography, is objective by utilizing quantitative parameters, enables the separate analysis of the functional behavior of the various renal compartments, and improves the differential diagnosis between parenchymatic dysfunction and pelvocalyceal obstruction.

Key words ^{99m}Tc-DTPA · Compartmental analysis · Renography · Parenchymatic dysfunction · Pelvocalyceal obstruction

G.A. Barbalias (✉) · E.N. Liatsikos
Department of Urology, University of Patras,
26500 Patras, Greece

G. Nikiforidis
Department of Medical Physics,
University of Patras, Patras, Greece

P. Vassilakos
Laboratory of Nuclear Medicine,
University of Patras, Patras, Greece

Introduction

The renogram is very useful in the diagnosis of renal dysfunction and obstructive uropathy. In classic renography the kidney is considered as a one-compartment system with the radionuclide presenting a uniform distribution throughout this compartment (isotropic model). However, calculating the parameters derived from the renal curve results in unclear and confusing information about the origin of the disorders. Indeed there are borderline cases where obstructive uropathy can be confused with parenchymatic dysfunction. Current progress in both the gamma-camera hardware and software has set the scene for the generation of time-activity graphs which can be further analyzed. This analysis leads to the extraction of quantitative parameters (slopes, peak times, integral activity, etc.), and therefore the interpretation of the renogram gains in objectivity [5].

Recently a successful approach in the diagnosis of renal diseases was achieved using deconvolution analysis of the renogram. Deconvolution is a mathematical technique which overcomes the influence of the tracer input curve on the renogram. This input curve depends on physiologic parameters not related to renal function and thus is considered as an unwanted component. The results of deconvolution yield the retention function, which represents the form of the renogram that would

be obtained if an injection were to be given directly into the renal artery [7, 9, 12–14, 17, 20, 21]. Various parameters are derived from the retention function but the most important is the mean transit time (MTT). These parameters are used as diagnostic indices, and show high sensitivity and specificity regarding abnormalities of function for the entire kidney. However, their application in the differential diagnosis between specific renal compartment disorders is limited, and thus they cannot be considered as definite differential diagnostic parameters. This may be due to the fact that these parameters are calculated through integrations and are strongly influenced by the renogram noise [10, 11, 15].

Several renal radionuclide techniques have been employed to estimate the radioisotope time-activity curves over different regions of the kidney. These techniques provide a more detailed study of the renal function before the mathematical analysis of the data.

The aim of this work was to determine characteristic and independent parameters related to the parenchyma and the pelvocalyceal system. This was made possible using compartmental analysis of tracer flow throughout the whole aortorenal component [2, 16, 19, 22, 24]. A specific tracer was selected, i.e., ^{99m}Tc-DTPA, for providing intrarenal kinetics allowing the implementation of a compartmental mathematical model leading to an analytically solvable system of differential equations. A protocol was formulated allowing the definition of regions of interest (ROIs) which were set over the suprarenal aorta, the entire kidney and the pelvocalyceal compartment [16]. The processing of the frames acquired in the various stages of the renogram enabled the determination of the flow coefficients of the above-mentioned renal compartments.

Materials and methods

A total of 60 individuals who were examined and investigated in the Department of Urology at the University of Patras formed three groups: group A consisted of 30 normals taken as controls, group B consisted of 15 patients with unilateral nephropathy (parenchymatic dysfunction) and group C consisted of 15 patients with unilateral obstructive uropathy (pelvocalyceal obstruction). All calculations inherent to renograms with ^{99m}Tc-DTPA were performed at the Department of Medical Physics. The mean age of the normal group was 37.5 years (range 18–65 years) with an equal sex distribution. The follow-up period ranged from 6 months to 2 years (mean 12 months) and the specific determination of pathology was achieved by appropriate methods (clinical examinations, urine cultures, biopsies, etc.).

All subjects imbibed 1 l of water 40 min before the onset of the renogram to ensure adequate hydration. Immediately after voiding they were placed supine with their back toward the scintillation camera (General Electric Starcam 2000 fitted with a low-energy all-purpose collimator) and positioned so that both kidneys and the abdominal aorta were located within the camera's useful field of view. One milliliter of DTPA solution labeled with 370 MBq of sodium pertechnetate ($NaTcO_4$) was prepared according to the manufacturer's instructions and injected as a bolus into the patient's antecubital vein. This standard radiation activity was administered to all subjects, regardless of their status, at the beginning of the examination. The data set consisted of 31 frames (1 frame/2 s) pertaining to the renal blood flow and 92 frames (1 frame/20 s) corresponding to renal function.

ROI were set up over the suprarenal aorta, the pelvocalyceal compartment and the entire kidney. The flagged areas of interest were selected by edge detection of the isotope concentration interactively with a joystick. The ROI over the suprarenal aorta was set up from early frames, and the ROI over the entire kidney was set from an image formed in the second minute after bolus administration [1, 18]. Finally the pelvocalyceal ROI was determined from the medial and last images of the renogram (separation of parenchyma from dilated calyces was achieved by superposing late pelvic pictures on the early views). The ROI over the bladder was set up from an image formed from the last frames where the volume of the bladder and the radioactivity concentration are at maximum. ROIs over the renal and bladder background were identified avoiding the region of the central vessels.

From the above ROIs, data regarding the radioisotope activity versus time were obtained. Renal parenchymal activity was derived by subtracting pelvocalyceal activity from that of the entire kidney [24]. These radioisotopic activities were corrected by subtracting ipsilateral background activity after size normalization of the ROIs [19]. In all cases the data of the renogram were filtered using smoothing spline functions in order to reduce both statistical noise and certain physiologic variations in radioisotope time activity [8].

For the analytic description of these experimental data we developed a six-compartment model with time-invariant parameters and variables (Fig. 1). It is assumed that our system follows linear kinetics, and since the volume of the renal compartments can be considered as constant, there is a steady flow and the mixing of the tracer in blood and urine is uniform.

The solution of this system provides the analytic form of the activity of the suprarenal aorta, the parenchyma and the pelvocalyceal compartment: $y_1(t)$, $y_2(t)$ and $y_3(t)$, respectively. Fitting the experimental data of each compartment to the corresponding analytic expression we determined the flow coefficients for the suprarenal aorta, parenchyma and pelvocalyceal compartment: k_1, k_2 and k_3, respectively [16].

To resolve the system of differential equations we suppose that the uniform mixing of the tracer in blood occurs instantly after the bolus injection. The six compartments correspond to the suprarenal aorta, left and right parenchyma, left and right pelvocalyceal compartment and finally the bladder (Fig. 1). The mathematical support of this model is given in the Appendix.

For further validation of the analysis we compared our data as analyzed by the deconvolution technique.

Results

In Tables 1 and 2 the results of classic renography for all patients are presented. The parameters used were the peak time and the excretion half-time. The analysis

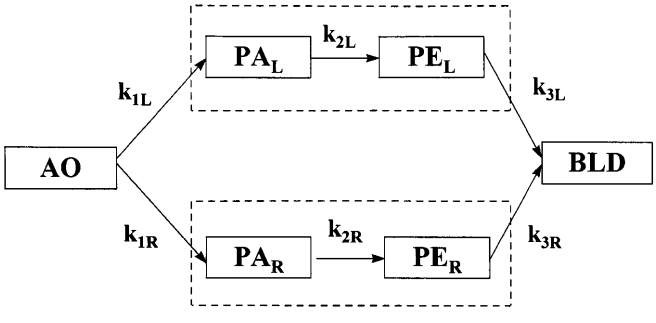

Fig. 1 Mathematical representation of the aortorenal system by a six-compartment system. The six compartments correspond to the suprarenal aorta (*AO*), left and right parenchyma (PA_L, PA_R), left and right pelvocalyceal compartment (PE_L, PE_R) and finally the bladder (*BLD*). The flow coefficients of the first four compartments are denoted by k_1, k_{2L}, k_{2R}, k_{3L} and k_{3R}, respectively

(unpaired t-test) showed a statistically significant difference in peak time for both groups of patients compared with the controls ($P < 0.05$). However, the difference between the same parameters of the two groups of patients is not statistically significant.

In Tables 3 to 6 the data are presented when the peak time and the excretion half-time are calculated separately in the parenchyma and the pelvocalyceal compartment. Following this approach the statistical analysis (unpaired t-test) shows an even more significant difference between patients and normals. Interestingly the statistical difference found between the parameters of the two groups of patients for both the parenchyma and the pelvocalyceal compartment was not significant. It is obvious that this approach cannot clearly distinguish between patients with parenchymatic dysfunction and those with pelvocalyceal obstruction.

Table 7 summarizes the MTT (derived by deconvolution analysis) of the parenchyma and the pelvocalyceal compartment of the three groups. It can be seen again that while there is very significant statistical difference in MTT between normals and patients this is strongly reduced when we compare parenchymatic dysfunction with pelvocalyceal obstruction. For brevity we have presented the typical procedure of deconvolution analysis regarding only the whole kidney (Fig. 2).

In Fig. 2 the curve fittings of typical data sets regarding the suprarenal aorta for (a) a normal subject, (b) a patient with parenchymatic dysfunction and (c) a patient with pelvocalyceal obstruction are presented.

In Figs. 3 and 4 the fittings of the parenchymatic and the pelvocalyceal radioactivity are given for the three groups. In all cases we used the parameter χ^2 as an estimator of the goodness of fit. We found that χ^2 for the

Table 1 The peak time (T_p) and excretion half-time ($T_{1/2}$) of the whole kidney in normals, patients with parenchymatic dysfunction and patients with pelvocalyceal obstruction

Group	n	T_p (min) (mean ± SD)	$T_{1/2}$ (min) (mean ± SD)
Normal	30	2.5 ± 1.1	11.9 ± 1.3
Parenchymatic dysfunction	15	6.8 ± 1.7	17.4 ± 1.9
Pelvocalyceal obstruction	15	6.0 ± 1.2	18.9 ± 2.3

Table 2 Statistical comparison of the peak time (T_p) and excretion half-time ($T_{1/2}$) of the whole kidney between normals, patients with parenchymatic dysfunction (*PD*) and patients with pelvocalyceal obstruction (*PO*)

Time	Normal–PD		Normal–PO		PD–PO	
	t_{43}	P	t_{43}	P	t_{28}	P
T_p	10.26	< 0.001	9.76	< 0.001	1.49	0.148
$T_{1/2}$	11.43	< 0.001	13.08	< 0.001	1.95	0.062

Table 3 The peak time (T_p) and excretion half-time ($T_{1/2}$) of the parenchyma in normals, patients with parenchymatic dysfunction and patients with pelvocalyceal obstruction

Group	n	T_p (min) (mean ± SD)	$T_{1/2}$ (min) (mean ± SD)
Normal	30	2.1 ± 0.9	11.5 ± 1.3
Parenchymatic dysfunction	15	6.4 ± 1.1	18.8 ± 3.9
Pelvocalyceal obstruction	15	5.3 ± 1.2	16.4 ± 2.8

Table 4 Statistical comparison of the peak time (T_p) and excretion half-time ($T_{1/2}$) of the parenchyma between normals, patients with parenchymatic dysfunction (*PD*) and patients with pelvocalyceal obstruction (*PO*)

Time	Normal–PD		Normal–PO		PD–PO	
	t_{43}	P	t_{43}	P	t_{28}	P
T_p	14.02	< 0.001	10.04	< 0.001	2.617	< 0.05
$T_{1/2}$	9.35	< 0.001	8.06	< 0.001	1.936	0.063

Table 5 The peak time (T_p) and excretion half-time ($T_{1/2}$) of the pelvocalyceal compartment in normals, patients with parenchymatic dysfunction (*PD*) and patients with pelvocalyceal obstruction (*PO*)

Group	n	T_p (min) (mean ± SD)	$T_{1/2}$ (min) (mean ± SD)
Normal	30	2.9 ± 0.8	12.3 ± 1.4
Parenchymatic dysfunction	15	8.2 ± 2.2	15.6 ± 2.4
Pelvocalyceal obstruction	15	6.4 ± 1.3	22.3 ± 3.6

Table 6 Statistical comparison of the peak time (T_p) and excretion half-time ($T_{1/2}$) of the pelvocalyceal compartment between normals, patients with parenchymatic dysfunction (*PD*) and patients with pelvocalyceal obstruction (*PO*)

Time	Normal–PD		Normal–PO		PD–PO	
	t_{43}	P	t_{43}	P	t_{28}	P
T_p	11.83	< 0.001	11.17	< 0.001	2.73	< 0.05
$T_{1/2}$	5.84	< 0.001	13.43	< 0.001	5.99	< 0.001

Table 7 Deconvolution analysis: mean transit times (MTT) of the parenchyma and the pelvocalyceal compartment of the three groups

Group	n	Parenchyma (mean ± SD)	Pelvocalyceal component (mean ± SD)
Normal	30	150 ± 48	80 ± 28
Parenchymatic dysfunction	15	414 ± 149	152 ± 59
Pelvocalyceal obstruction	15	374 ± 118	248 ± 108

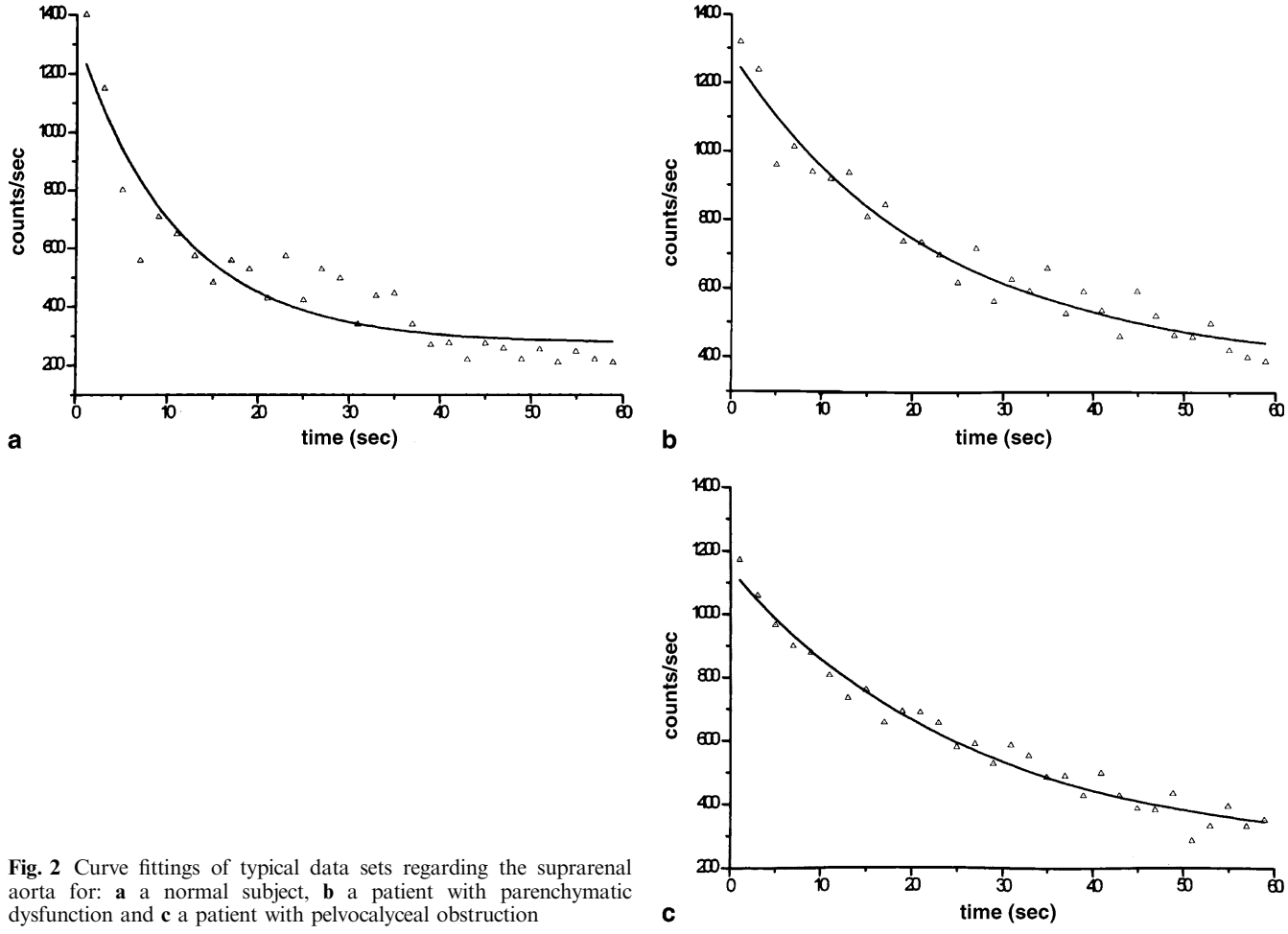

Fig. 2 Curve fittings of typical data sets regarding the suprarenal aorta for: **a** a normal subject, **b** a patient with parenchymatic dysfunction and **c** a patient with pelvocalyceal obstruction

fittings of the suprarenal aorta curve are lower than that for the parenchymatic and pelvocalyceal radioisotope curve. [χ^2 (ranging between 1.2 and 3.0) indicates a good fit.] The fittings were performed using the software package Mathematica [8, 23].

Tables 8 and 9 summarize the mean values and standard deviations of the flow coefficients for the suprarenal aorta, the parenchyma and the pelvocalyceal compartment of the three groups. The differences between the aorta flow coefficients (k_1) are statistically significant not only between normals and patients but also between patients with parenchymatic dysfunction and those with pelvocalyceal obstruction. The same differences are observed comparing the pelvocalyceal coefficients (k_3) of all three groups. As regards the parenchymal coefficients (k_2) we found significant differences ($P < 0.05$) between normals and patients which were not significant when the two groups of patients were compared.

Discussion

The kidney is a system composed of more than one component and it follows that its radioactivity curve contains overlapping information from both the parenchyma and the pelvocalyceal compartments [5, 15, 24]. Calculating the parameters derived from the whole kidney curve results in unclear information about the origin of disorders, and furthermore there are cases where obstructive uropathy can be confused with parenchymatic dysfunction [11, 15].

According to many researchers there is no "gold standard" in the diagnosis of obstruction [3]. Each of the three best known alternative methods – the Whitaker test, diuresis renography and measurement of MTT – has certain disadvantages. Pressure flow studies are invasive and employ infusion rates well in excess of physiologic rates of urine production, and falsely low pressures may also occur [4]. In diuresis renography some kidneys with poor function may fail to respond to the diuretic and a further limitation of this method is that in grossly dilated kidneys results may be equivocal [15]. The furosemide administration in diuresis renography influences the renography curve from one point of the curve onward. In compartmental analysis, though, furosemide administration has further consequences in the mathematical evaluation and calculations of the parameters concerning all the renal compartments. Another point against using a diuretic has to do

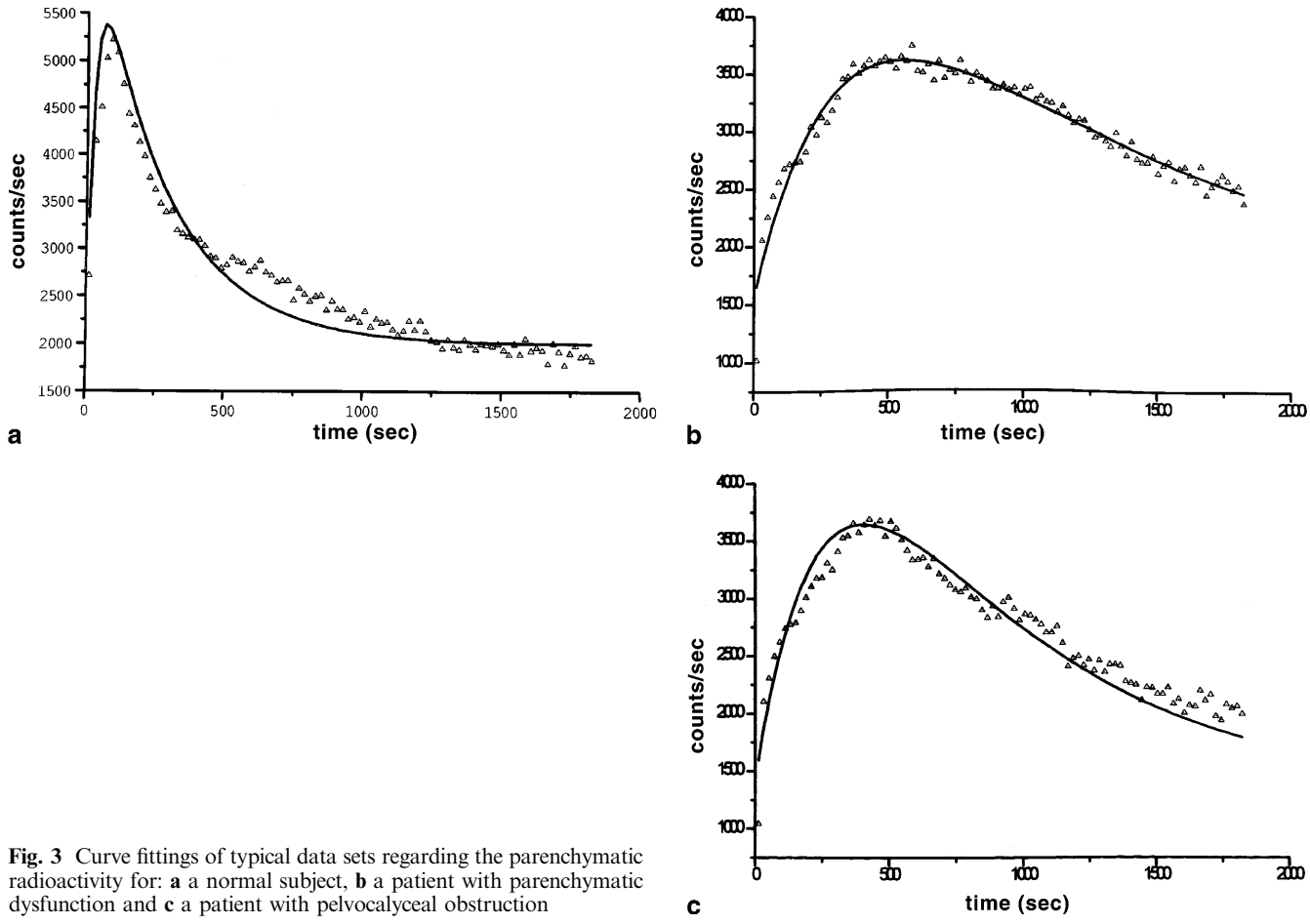

Fig. 3 Curve fittings of typical data sets regarding the parenchymatic radioactivity for: **a** a normal subject, **b** a patient with parenchymatic dysfunction and **c** a patient with pelvocalyceal obstruction

with the definition of ROIs, which becomes even more problematic. Recently several studies have emphasized MTT estimation, using deconvolution analysis. These studies indicate that the use of MTT, T_{80}, T_{20}, etc., in the distinction between the normal and abnormal kidney is of great value [7, 9, 14, 17], but so far the role of MTT in the differentiation of obstructive uropathy from parenchymatic dysfunction has not been adequately elucidated [11, 15].

Our results, when compared with those of classic renography, deconvolution analysis and those from the empirical analysis of tracer time activities over the parenchyma and the pelvocalyceal compartment, taken separately, clearly show a distinct improvement. This improvement underlines an increase in the differential diagnosis potential of this methodology between parenchymatic and obstructive dysfunction.

Using the standard deviation (SD) of the random value of our samples, and as cutoff values the points $x + 2$ SD, the sensitivity of the methodology can be determined (positive test given that the examined individual is a patient) when its specificity (negative test given that the examined individual is not a patient) is 95%.

Analyzing the results we conclude that the sensitivity of the four different methods (classic renography, empirical analysis, deconvolution analysis, compartmental analysis) regarding the differentiation between normals and patients is 90%, 95%, 99% and more than 99%, respectively. The differential diagnosis potential between parenchymatic dysfunction and obstructive uropathy, given by previous methodologies of classic renography, empirical analysis and deconvolution analysis, proved to be low compared with that provided by our proposed methodology (reaching 90%). This improved differentiation ability of compartmental analysis is due exclusively to the mathematical model used, since a similar technique of data acquisition was used as in the alternative radionuclide methods.

Indeed, the parameters derived from the empirical analysis of the corresponding curves of the parenchymatic and the pelvocalyceal component (peak time, transit time, etc.) are not purely characteristic of the function of each compartment and still continue to present a significant overlap in their function. Thus, it is obvious that a dysfunctional problem of the pelvocalyceal compartment will interfere with the parenchymatic time activity and, conversely, a parenchymatic defect will be reflected in the time activity of the pelvocalyceal compartment.

On the contrary, applying compartmental analysis and following a stepwise technique we are able to

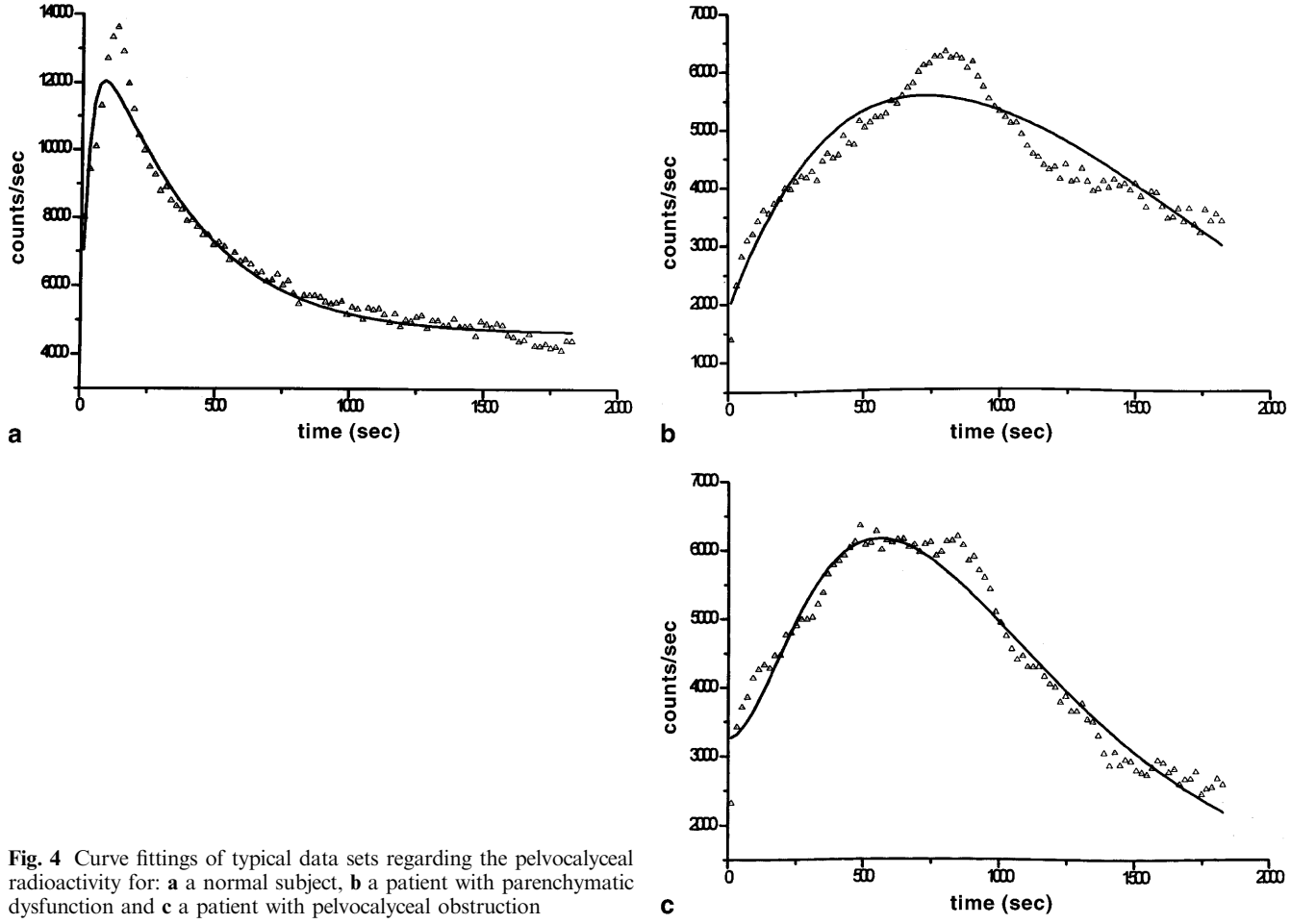

Fig. 4 Curve fittings of typical data sets regarding the pelvocalyceal radioactivity for: **a** a normal subject, **b** a patient with parenchymatic dysfunction and **c** a patient with pelvocalyceal obstruction

Table 8 Mean values and standard deviations of the flow coefficients of the suprarenal aorta (k_1), the parenchyma (k_2) and the pelvocalyceal compartment (k_3) in normals, patients with parenchymatic dysfunction and patients with pelvocalyceal obstruction

Group	n	$k_1 \times 10^4$ (mean ± SD)	$k_2 \times 10^4$ (mean ± SD)	$k_3 \times 10^4$ (mean ± SD)
Normal	30	773.0 ± 43.0	30.0 ± 4.0	442.0 ± 137.0
Parenchymatic dysfunction	15	42.0 ± 2.8	10.1 ± 1.5	46.8 ± 11.1
Pelvocalyceal obstruction	15	308.0 ± 103.0	11.6 ± 3.1	5.7 ± 2.0

Table 9 Statistical comparison of the flow coefficients of the suprarenal aorta (k_1), parenchyma (k_2) and pelvocalyceal compartment (k_3) in normals, patients with parenchymatic dysfunction (*PD*) and patients with pelvocalyceal obstruction (*PO*)

Flow coefficient	Normal–PD	Normal–PO *P* value	PD–PO
k_1	< 0.001	< 0.001	< 0.001
k_2	< 0.001	< 0.001	**0.103**
k_3	< 0.001	< 0.001	< 0.001

determine the flow coefficients of each compartment (suprarenal aorta, parenchymatic and pelvocalyceal compartments) which are compartment-characteristic parameters. All the above parameters are independent, and can be used in combination for the differential diagnosis related to each compartment. Furthermore, applying multivariate analysis the overall sensitivity of our method could be further improved.

We chose to use ^{99m}Tc-DTPA in this study since it is known that dynamic renal studies with this radionuclide yield results that are amenable to analysis by the method of mathematical compartmental analysis, as the DTPA is cleared in a truly glomerular manner by the kidneys. It is pointed out that there are various alternative compartmental models for the radionuclide kinetics that can lead to large differences. Considering the renal system as a model of six compartments is appropriate for the analytical description of DTPA metabolism. This choice is dictated not only by the anatomic and functional substrate of the kidney but also by the technical limitations inherent to the gamma-camera.

It should be noted that the real biologic system is complex and the physiologic correspondence with our model should be considered an approximation. Additionally there are measurement limitations which need to be considered. With the scintillation camera the kidney

can be delineated in its coronal plane, where regional separation of the organ may be attempted. However, since the resolution of the scintillation camera is of the order of 1 cm at best, the cortical and medullary functions cannot be separated. Analysis of the regional physiology of the kidney has been attempted from time-activity curves of the renal parenchyma and renal pelvis, but satisfactory separation of these areas is sometimes questionable. As described above we selected ROIs on the frame corresponding to the maximum activity of the renal compartments. The late onset of activity in the renal pelvis makes the setting up of a ROI over the pelvis much easier but the separation of the parenchyma from the renal pelvis may be difficult, since ROI determination is based on a subjective visual assessment. It is also known that the pelvis may be intrarenal and the radiation from the pelvis may overlap the parenchymatic area especially in the dilated upper urinary tract [6]. Also, high count rate activity originating in the renal pelvis may contribute to activity seen in the parenchyma.

The dynamic pattern of tracer activity over the kidney may be influenced by many factors other than the function of this organ. Quality of bolus injection, systematic recirculation of the tracer and multicompartmental removal of blood pool activity are factors that may potentially alter or distort the temporal pattern of renal activity. Nevertheless the errors introduced by the aforementioned limitations are small and should therefore be considered negligible in clinical applications.

Conclusion

The proposed method attempts to clarify the information given by renography, utilizing the basic mechanisms that govern renal function and applying relatively simple mathematics. This investigation may be useful to establish or confirm the diagnosis of obstruction, to ascertain its localization or to determine its extent and severity.

Furthermore, our data indicate that this methodology increases the sensitivity of renography, is objective by utilizing quantitative parameters, enables the separate analysis of the functional behavior of the renal compartments and finally improves the differential diagnosis between parenchymatic dysfunction and pelvocalyceal obstruction.

Appendix

The appropriate differential equations that describe the model are as follows [2, 19, 24]:

$$\frac{dy_1}{dt} = -k_1 y_1 \tag{1}$$

$$\frac{dy_{2L}}{dt} = k_{1L} y_1 - k_{2L} y_{2L} \tag{2}$$

$$\frac{dy_{2R}}{dt} = k_{1R} y_1 - k_{2R} y_{2R} \tag{3}$$

$$\frac{dy_{3L}}{dt} = k_{2L} y_{2L} - k_{3L} y_{3L} \tag{4}$$

$$\frac{dy_{3R}}{dt} = k_{2R} y_{2R} - k_{3R} y_{3R} \tag{5}$$

$$\frac{dy_4}{dt} = k_3 y_4 \tag{6}$$

where $y_i(y_i(t))$ are the decay-corrected radioactivity in the various compartments, and k_i are flow constants for the transport of tracer between compartments.

It is assumed that at zero time $t = 0$, $y_1 = y_0$, where y_0 is the maximum radioactivity in the suprarenal aorta. This is a good approximation for normal and abnormal cases with normal uptake.

Resolving the system we obtained respectively the renal input, the parenchymal, pelvic and bladder activity/time functions:

$$y_1(t) = y_{1,0}\, e^{-k_1 t} \tag{7}$$

$$y_{2L}(t) = e^{-k_{2L}t}\left\{\frac{(k_{2L}-k_{1L})y_{2L,0} - k_{1L}y_{1L,0}}{(k_{2L}-k_{1L})} + \frac{k_{1L}y_{1L,0}}{(k_{2L}-k_{1L})} e^{(k_{2L}-k_{1L})t}\right\} \tag{8}$$

$$y_{2R}(t) = e^{-k_{2R}t}\left\{\frac{(k_{2R}-k_{1R})y_{2R,0} - k_{1R}y_{1R,0}}{(k_{2R}-k_{1R})} + \frac{k_{1R}y_{1R,0}}{(k_{2R}-k_{1R})} e^{(k_{2R}-k_{1R})t}\right\} \tag{9}$$

$$y_{3L}(t) = e^{-k_{3L}t}\left\{y_{3L,0} - \frac{k_{2L}A_L}{k_{3L}-k_{2L}}\left[1 - e^{(k_{3L}-k_{2L})t}\right] - \frac{k_{2L}B_L}{k_{3L}-k_{1L}}\left[1 - e^{(k_{3L}-k_{1L})t}\right]\right\} \tag{10}$$

$$y_{3R}(t) = e^{-k_{3R}t}\left\{y_{3R,0} - \frac{k_{2R}A_R}{k_{3R}-k_{2R}}\left[1 - e^{(k_{3R}-k_{2R})t}\right] - \frac{k_{2R}B_R}{k_{3R}-k_{1R}}\left[1 - e^{(k_{3R}-k_{1R})t}\right]\right\} \tag{11}$$

where

$$A_L = \frac{(k_{2L}-k_{1L})y_{2L,0} - k_{1L}y_{1L,0}}{(k_{2L}-k_{1L})}, \quad B_L = \frac{k_{1L}y_{1L,0}}{(k_{2L}-k_{1L})}$$

$$A_R = \frac{(k_{2R}-k_{1R})y_{2R,0} - k_{1R}y_{1R,0}}{(k_{2R}-k_{1R})}, \quad B_R = \frac{k_{1R}y_{1R,0}}{(k_{2R}-k_{1R})}$$

$$y_4(t) = y_{4L,0}e^{k_{3L}t} + y_{4R,0}e^{k_{3R}t} \tag{12}$$

References

1. Al-Nahhas A, Marcus AJ, Bomanji J, Nimmon CC, Dacie JE, Britton KE (1989) Validity of the mean parenchymal transit time as a screening test for the detection of functional renal

artery stenosis in hypertensive patients. Nucl Med Commun 10:807
2. Berman M (1977) Kinetic models for absorbed dose calculation. MIRD pamphlet no. 12. Society of Nuclear Medicine, New York
3. Bratt CG, Aurell M, Erlandson BE, Nilson AE, Nilson S (1982) Intrapelvic pressure and urinary flow rate in obstructed and non obstructed human kidneys. J Urol 127:1136
4. Britton KE, Whitfield HN, Nimmon CG, Hendry WF, Wickham JEA (1974) Obstructive nephropathy: successful evaluation with radionuclides. Lancet 1:905
5. Britton KE, Maisey MN (1983) Renal radionuclide studies. In: Maisey MN, Britton KE, Gilday DL (eds) Clinical nuclear medicine, 1st edn. Chapman & Hall, London pp 93–98
6. Cloutier RJ, Watson EE, Rohner RA, Smith EM (1972) Calculating the radiation dose to an organ. J Nucl Med 14:53
7. Diffey BL, Hall FM, Corfield JR (1976) The ^{99m}Tc-DTPA dynamic renal scan with deconvolution analysis. J Nucl Med 17:352
8. Fleming JS, Kenny RW (1977) A comparison of techniques for the filtering of noise in the renogram. Phys Med Biol 22:359
9. Frokiaer J, Jensen FT, Djurhuus JC, Christiansen PM, Harving N, Mortensen J (1990) The impact of unilateral obstruction on pelvic and parenchymal transit times in the pig kidney. Eur J Nucl Med 16:349
10. Gullquist RR, Fleming JS (1987) Error analysis by simulation studies in renography deconvolution. Phys Med Biol 32:383
11. Harper MD, Lecklitner M (1985) Quantitative evaluation of differential renal function: a new approach. J Nucl Med 26:647
12. Juni JE, Thrall JH, Froelich JW, Wiggins RC, Campbell DA Jr, Tuscan M (1988) The appended curve technique for deconvolution analysis: method and validation. Eur J Nucl Med 14:403
13. Kempi V, Sutton DG (1995) Estimating the diagnostic yields resulting from renography and deconvolution parameters: a logistic regression analysis. J Nucl Med 36:147
14. Lupton EW, Lawson RS, Shields RA, Testa HJ (1984) Diuresis renography and parenchymal transit times in the assessment of renal pelvic dilatation. Nucl Med Commun 5:451
15. Neal DE, Simpson W, Bartolomew P, Keavy PM (1985) Comparison of dynamic computer tomography, diuresis renography and DTPA parenchymal transit time in the assessment of dilatation of the urinary tract. Br J Urol 57:515
16. Nikiforidis G, Vassilakos P, Karatrandou A, Barbalias G (1995) In vivo estimation of radiation dose in renal pelvis and parenchyma during renography. Nucl Med Commun 16:47
17. Piepsz A, Ham HR, Erbsmann F, Hall M, Diffey BL, Goggin MJ, Hall FM, Miller JA, Lumbroso J, Di Paola R, Bazin JP, Di Paola M, Fries D (1982) A co-operative study on the clinical value of dynamic renal scanning with deconvolution analysis. Br J Radiol 55:419
18. Russell D (1993) Optimum sample times for single injection, multisample renal clearance methods. J Nucl Med 34:1761
19. Strand SE, Zanzonico P, Johnson TK (1993) Pharmacokinetic modeling. Med Phys 20:515
20. Sutton DG, Kempi V (1992) Constrained least-squares restoration and renogram deconvolution: a comparison by simulation. Phys Med Biol 37:53
21. Whitfield HN, Britton KE, Hendry WF, Nimmon CC, Wickham JEA (1978) The distinction between obstructive uropathy and nephropathy by radioisotope transit times. Br J Urol 50:433
22. Wolf IH, Buttermann G, Pabst HW (1978) Determination of total, divided and regional tubular clearance and excretion by compartmenral analysis of camera renograms. Contrib Nephrol 11:50
23. Wolfram S (1991) Mathematica: a system for doing mathematics by computer, 2nd edn. Addison-Wesley, Reading, Mass
24. Wooten WW (1983) Radionuclide kinetics in MIRD dose calculations. J Nucl Med 24:621